

Sketch-based Registration of 3D Cine MRI to 4D Flow MRI

Samin Sabokrohiyeh*

University of Calgary
Calgary, AB

Samin.Sabokrohiyeh@ucalgary.ca

Kathleen Ang

University of Calgary
Calgary, AB

kdang@ucalgary.ca

Mohammed Elbaz

University of Calgary
Calgary, AB

mohammed.elbaz@ucalgary.ca

Faramarz Samavati

University of Calgary
Calgary, AB

samavati@ucalgary.ca

ABSTRACT

Cardiac 4D Flow magnetic resonance imaging (4D Flow MRI) is a recent powerful technology that uniquely enables in-vivo acquisition of time-varying volumetric blood flow velocity field information in the three spatial dimensions over the cardiac cycle. Hence, 4D Flow MRI has emerged as an important medical diagnostic tool for evaluation of blood flow alteration in the heart chambers and great vessels. A critical requirement for accurate quantification and visualization of blood flow within the different heart chambers (e.g. the left ventricle (LV)) is the accurate anatomical context of cardiac chambers, which is missing in the 4D Flow MRI data. To tackle this problem, recent studies have proposed fusing the 4D Flow data with a complementary anatomical MRI scan (short axis 3D (multiple 2D slices) cine SSFP) through registration. However, since image registration is a non-linear optimization problem, the registration is slow and may not be accurate (e.g. the left ventricle can be incorrectly aligned to the right ventricle). To improve the registration performance and accuracy, localization techniques can be used. In this paper, we propose two sketch-based methods for effective localization of 4D Flow MRI to 3D cine MRI registration. We evaluate these methods and compare them with other localization methods.

CCS Concepts

• Applied computing → Life and medical sciences.

Keywords

Registration; localization; sketch-based interaction; 4D Flow MRI.

1. INTRODUCTION

Cardiac magnetic resonance (CMR) imaging plays an important role in the diagnosis of heart diseases, which is vital in the treatment of such diseases. Cardiac 4D Flow magnetic resonance imaging (4D Flow MRI) is a recent technology that enables 4D (3D+time) imaging of a volumetric blood flow velocity field over the cardiac

SAMPLE: Permission to make digital or hard copies of all or part of this work for personal or classroom use is granted without fee provided that copies are not made or distributed for profit or commercial advantage and that copies bear this notice and the full citation on the first page. To copy otherwise, or republish, to post on servers or to redistribute to lists, requires prior specific permission and/or a fee.

Conference'10, Month 1–2, 2010, City, State, Country.

Copyright 2010 ACM 1-58113-000-0/00/0010 ...\$15.00.

DOI: <http://dx.doi.org/10.1145/12345.67890>

cycle. Blood flow behavior can be obtained by processing and analyzing the flow information provided by 4D Flow MRI data, which can be used for quantification and visualization of flow features such as vorticity, flow speed, and turbulent kinetic energy. Flow assessment can be advantageous in evaluating heart function, thus assisting in a better diagnosis [8]. There have been several studies quantifying and evaluating blood flow, specifically in different regions of the heart (e.g. flow in the left ventricle, right ventricle, left atrium, etc.) for better understanding and evaluation of various cardiac pathophysiology [7]. In particular, flow in the left ventricle of the heart can help in the diagnosis of heart abnormalities and disorders such as left ventricle wall motion disorders, valvular disease and arrhythmia [10].

A typical 4D Flow MRI dataset of a single subject is composed of four time-varying volumetric datasets: the components of the velocity field in three different spatial directions (i.e. x, y, and z) and magnitude images as a reference for the anatomy [24]. Due to the poor quality of the magnitude images, visualization and quantification of the velocity field are difficult to obtain with respect to anatomical context [37]. Alternatively, 3D cine MRI (short-axis 3D (multi 2D slice) SSFP cine MRI), a complementary dataset which is commonly acquired in the same scanning session, provides high quality anatomical information [37]. (Of note, throughout the text “3D cine MRI” refers to multi 2D slice cine MRI.) Short-axis 3D cine MRI can capture the anatomical structure of the heart more clearly, since the images have higher resolution and contrast [36]. In addition, there are several reliable and accurate segmentation techniques using 3D cine MRI data [14]. These two datasets (4D Flow MRI and 3D cine MRI) can be fused to take advantage of the strengths of each. Data from 3D cine MRI can provide high-quality anatomical context for the 4D Flow dataset, for example, or even a segmentation from 3D cine MRI can be used to segment flow data from 4D Flow MRI. Therefore, we desire to align these two datasets using an accurate registration.

Registration is widely used in the medical field with the purpose of aligning two or more different datasets [6, 13, 20]. This data fusion can be done by finding a transformation matrix that spatially aligns one image to another. Finding the transformation matrix for the best alignment between the datasets is formulated as an optimization problem. For the fitness function, we use mutual information, which provides the relation between intensities [20]. This optimization is non-linear and should be solved using iterative methods.

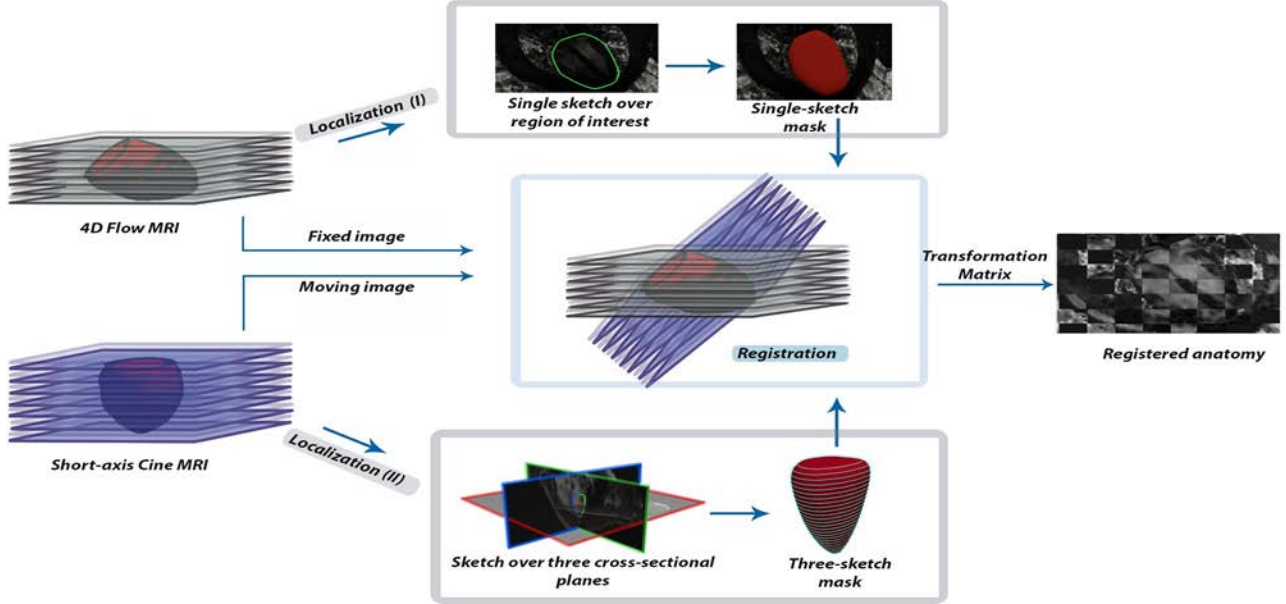


Figure 1. Diagram of the developed method (registration can be done by choosing one of the localization techniques to provide the mask).

One of the crucial requirements of an accurate registration is to localize the data to a specific region, which reduces the time needed for registration by constraining the search space. Furthermore, localization reduces the impact of noise and prevents the alignment of unwanted organs and artifacts visible in the image [20]. There are several works which have used registration (specifically of cine SSFP to 4D Flow MRI) to accurately quantify energy loss, kinetic energy, vorticity, etc. [9, 11, 12, 18, 19]. In all of these studies, they obtain a manual segmentation prior to registration, but providing such segmentations is tedious and time-consuming. One recent work [15] employed rigid in-plane slice-to-volume registration of breath-hold cine bSSFP (balanced steady-state free precession) to 4D Flow MRI. Their goals were to correct motion misalignments in the breath-hold MR images and to provide a segmentation for the 4D Flow MRI dataset (i.e. a transferred manual segmentation from the cine bSSFP images). This study used an automatic cropping system with a box around the whole heart to localize their data, which may not work for all kinds of data and consequently requires a visual check [17].

In this paper, we use a sketch-based localization method for improving registration quality. To construct the localized region, we developed two slightly different sketch-based methods: (1) we use a single sketch on the 4D Flow MRI and convert it to a localizing mask, and (2) we provide a more accurate region of interest by drawing three sketches on three intersecting planes. A rigid volume-to-volume registration is then executed, using normalized mutual information as a similarity metric [28]. After registration, we obtain a transformation matrix, which transforms the anatomy information from the 3D cine MRI data to the 4D Flow MRI data. One interesting observation from our work is that the localization mask from one time frame can be applied for registration of other time frames.

Fig. 1 depicts the overall method developed. The input is the 4D Flow MRI data and the 3D cine MRI data corresponding to the 4D Flow MRI. The localization process can be done by using one rough sketch over the 4D Flow MRI to define a mask for registration, or by using three sketches over the 3D cine MRI data to construct the localization mask. The output is the transformation

matrix between the 3D cine MRI and the 4D Flow MRI, which can transfer the anatomical structure information to the 4D Flow MRI. Furthermore, the localization mask constructed using our method on one time frame can potentially be used for registration of subsequent time frames.

To evaluate our registration results, we quantitatively compare the registration accuracy using different localization masks with four different geometric metrics. The results show that the quality of registration using our sketch-based localization is comparable to registration using the manual segmentation (ground truth) as the localization mask.

In summary the main contribution of this work is to introduce a sketch-based localization method for improving time-varying 3D cine MRI to 4D Flow MRI registration. The improvement can be seen in the run time performance and/or the accuracy of the registration.

Section 2 covers background information about 4D Flow MRI, registration, and related sketch-based interaction work in medical applications. In Section 3 we describe the methodology in two main steps: localization and registration, Section 4 discusses the evaluation of our method and some results, and Section 5 concludes with a discussion of potential future work.

2. BACKGROUND AND RELATED WORK

4D Flow MRI magnitude images provide the anatomical structure of the heart in addition to the blood flow information. However, due to the narrow intensity range of these magnitude images, even expert clinicians have difficulty delineating the heart structure visually [8]. On the other hand, cardiac 3D cine MRI (which contains a stack of 2D slices intersecting the heart and can be obtained within the same scan session) captures the cardiac anatomy with higher resolution and clarity. Thus, although this sequence does not provide blood flow information, the data resulting from 3D cine MRI can be used to identify the heart chambers more accurately. To integrate these two datasets, image registration can be used.

Image registration has a long history in medical applications as it leads to more accurate diagnosis [6, 13, 20]. There is a rich body of literature on fusing data from different modalities such as Computed Tomography (CT), magnetic resonance (MR), Xray, ultrasound, etc [16]. In general, image registration techniques can be classified in two main categories: landmark-based and intensity-based. Landmark-based registration methods commonly use geometric features such as corresponding landmarks, edges, surfaces, etc. to align two datasets [29]. However, defining features in complex images such as cardiac MRI is not simple. Defining the accurate corresponding landmarks and geometric features in two different modalities is challenging and the correspondence may not exist. Indicating inaccurate corresponding features may affect the result of the registration [22]. On the other hand, intensity-based registration techniques try to find the best alignment based on finding a relationship between the intensities of two datasets. There are many intensity-based similarity metrics such as mean squared difference, normalized cross correlation, and normalized mutual information [20]. In recent research on registering 4D Flow MRI and morphological cine MRI [15], normalized mutual information yielded higher geometric accuracy compared to normalized cross correlation and was therefore chosen as the registration technique used in our work.

There have been several recent works that used registration of 3D cine MRI to 4D Flow MRI in order to measure flow parameters [9, 11, 12, 18, 19]. One important component of registration is localization, which reduces the impact of noise and improves the quality of registration by defining a suitable search space. In these studies, manual segmentations were provided prior to registration; however, providing such segmentations is time-consuming even for an expert clinician. To sketch over all slices in every time step would soon become tedious – for instance, to segment the left ventricle alone would require sketching over almost 15 slices per time frame, and a typical dataset over one cardiac cycle may have around 30 time frames. In another recent work [15] on registering 4D Flow MRI to breath hold cine MRI, a box was used as a localization mask around the heart. They used an automatic system for cropping the region of interest around the heart, which has some potential drawbacks: in cases with small hearts, finding the centroid is challenging and therefore the location of the heart is hard to detect, and in cases with large hearts, some parts may be cut out due to the cropping. Thus, a visual check is essential for this approach [17]. We aim to overcome some of these limitations by introducing a sketch-based interface for localization.

A number of studies have shown that incorporating sketch-based interfaces in medical applications is helpful. For instance, a sketch-based method for defining a region of interest has been developed to obtain an interactive volume segmentation [3]. Freehand sketches provided by the user are used to cut the 3D volume based on a seeded region growing method. Parts of the volume outside the sketch are cut and this process can be repeated to obtain the user's desired region of interest in an interactive way. Volume segmentation can also be done by pre-processing the user's input sketches (e.g. contours, clicks, etc.) in the 2D domain and converting it to 3D using the Volume Catcher system [27]. Some sketch-based tools have also been developed for exploring the hidden parts of the data such as cutting, peeling, layering, and drilling [2]. The user can also draw a curve over the 3D volume, which is used to define a region that the user wants to uncover. These tools are helpful for discovering complex volumetric data which suffer from occlusion. By removing outer parts of the data, one can explore the inner structure in a more efficient way. In the context of contouring over 2D slices, Zhou and Xie [39] developed

an interactive tool that uses a snake model and multi-scale curve editing to improve the segmentation drawn by the user. SmartPaint [23] is another interactive tool for segmentation of medical images. The user sweeps the mouse cursor over the region of interest and the final selection is determined based on the intensity and Euclidean differences between the voxels nearby and the center of the brush. However, although these interactive tools can improve the quality of the manual segmentation, they still require contouring slice by slice over all slices, which is still time consuming.

3. METHODOLOGY

To take advantage of both 3D cine MRI and 4D Flow MRI, one can fuse these two datasets using registration. This registration is not a trivial task due to the noise in the data and also the possibility of misalignment (e.g. right ventricle to left ventricle). For this purpose we introduce a sketch-based method for localization prior to registration.

3.1 Localization

For localization, various approaches can be used (see Fig. 2). In the most extreme case, no additional localization information is given – in this case, the bounding volume of the data effectively serves as a localization mask. As another example (which was discussed previously), one can use a cropping box to define the region of interest [15]. If the 3D cine MRI has already been segmented, one of the segmentations (e.g. left ventricle) can be used for localization. This results in a good quality registration with less running time needed as compared to using no mask (which will likely lead to an incorrect registration). Unfortunately, conventional segmentation of cardiac medical images is not always available and is not always easy to obtain [33]. Therefore, our goal is to provide an efficient and effective localization mask even when there is no prior segmentation. Specifically for the localization, there are some criteria to be considered:

- 1) The localization mask should perform as well as the accurate manual segmentation mask, but we do not want it to be as expensive and tedious to obtain.
- 2) A smaller localization mask is preferred as a large bounding volume generally requires a lot of computation time and/or can lead to misalignment.
- 3) Very small localization masks may miss important and unique features which can lead to misalignment.

We propose the use of sketch-based interfaces to provide a rough segmentation around a suitable region. Such a region could be, for instance, the entire heart, left ventricle, or right ventricle; we refer to this region as the region of interest (ROI). Inspired by the work of Cherlin et al. [5] on creating 3D shapes with only a few strokes, we use only a few sketched contours to create our localization masks.

Specifically, we propose two sketch-based techniques for creating a localization mask: (1) a rough single-sketch interface for fast mask creation, and (2) a three-sketch interface for creating a more accurate mask using three perpendicular anatomical image planes. The user is required to provide only one mask on the diastolic time frame (the time frame that the heart is at its largest size). Empirically, we found that using this mask alone is sufficient for the rest of the time frames, perhaps because the ROI remains within or near the original localization over the entire cardiac cycle.

The single-sketch technique is intended for defining larger ROIs such as the whole heart. In this technique, the user can provide one rough sketch over the region of interest, which defines the cross section curve. Extruding this curve along a defined line segment

Using no mask	Cropping box	Single-sketch	Three-sketch	Manual segmentation	Small region
<ul style="list-style-type: none"> Very high Processing time No user input Sensitive to noise More probable wrong registrations 	<ul style="list-style-type: none"> High processing time No user input Sensitive to noise Possible misalignments 	<ul style="list-style-type: none"> Average processing time Input one sketch Not sensitive to noise No misalignments 	<ul style="list-style-type: none"> Low processing time Input three sketches Not sensitive to noise No misalignments 	<ul style="list-style-type: none"> Low processing time Contouring over all slices of the data Not sensitive to noise No misalignments 	<ul style="list-style-type: none"> Very low processing time Input one+ sketch More probable wrong registrations (misses important features)

Figure 2. Comparison between different masking schemes

creates a sweep surface [5]. Here we define this line segment as a straight line perpendicular to the cross section's center and contained within the volume of the 4D Flow MRI (Fig. 3). This binary mask can then be used to localize and confine the heart for an efficient registration of the 3D cine MRI to the 4D Flow MRI. The single-sketch technique can be done using either the 4D Flow MRI or the 3D cine MRI since the extent of the whole heart is observable in both scans.

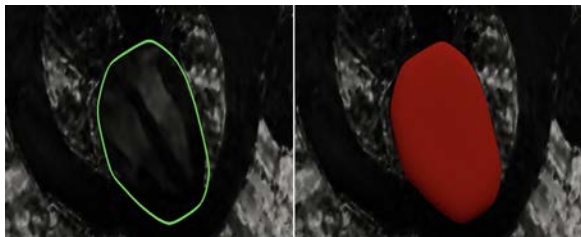


Figure 3. Bounding volume created from the sketch for registration purposes.

The three-sketch technique is intended for defining smaller ROIs, such as a specific chamber of the heart. This requires sketching over the 3D cine MRI images, since detailed anatomical structures are more visible in these images. In this technique (using three sketches), the user is provided with three images corresponding to three intersecting planes of the 3D cine MRI data. By default, the three cross-sectional planes are oriented such that one plane corresponds with the short-axis 3D cine MRI, the second plane corresponds with the long-axis view, and the third plane corresponds with a four chamber view. (The second and third planes are perpendicular to the first.) After the planes have been defined, freehand sketches over the ROI on each of the three cross-

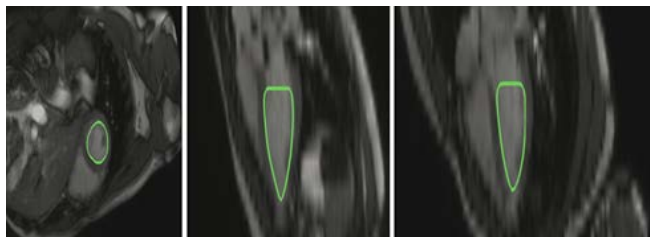


Figure 4. Sketches provided by the user over the left ventricle on the 3D cine MRI.

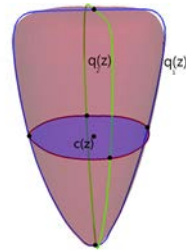


Figure 5. Three sketches for constructing the cross sectional blending surface.

sectional planes can be drawn to define its boundaries. As an example, the sketches over the left ventricle (chosen ROI) are shown in Fig. 4.

Once the three sketches have been made, we reconstruct a three-dimensional surface that can be used as a localizing mask for the volumetric data. To mathematically form the surface out of the sketches, a cross sectional blending construction method is used. A cross sectional blending surface can be constructed by finding a centerline from the two vertical sketches, and then sweeping a cross section along that line. The cross section curve is scaled based on its intersection with the two vertical curves such that it has four intersection points (i.e. two on each curve) at each height value. Let $q_1(z)$ and $q_2(z)$ (Fig. 5) be our two vertical curves, and let $c(z)$ be the center point of these two curves at each z value that we want to move the cross section curve along. For each z value, we center the cross section curve at $c(z)$ and scale it to pass through $q_1(z)$ and $q_2(z)$ [5]. The contours formed by following this method are seen in Fig. 6.

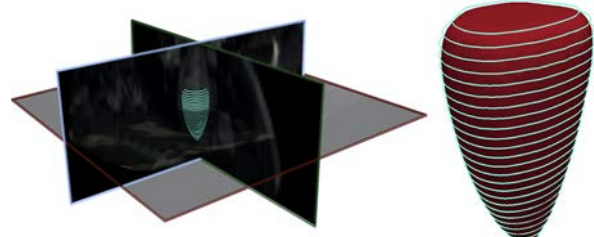


Figure 6. Contours of the cross sectional surface.

3.2 Registration

In order to simplify the identification and processing of important components of the heart from 4D Flow MRI data, one can use image registration (which has been widely used to integrate information from different medical images [25]) to map the anatomy from 3D cine MRI images to 4D Flow MRI images. Image registration is the process of finding the best match alignment between two sets of images. The result is a transformation matrix that maps one image (or set of images) to another. Registration techniques can be divided into two main categories: intensity-based and feature-based. Since feature-based registration requires extraction of features from both scans, intensity-based registration was deemed to be a better approach for this problem.

We use an intensity-based method that attempts to find a relationship between the intensities in two images in order to align them [38]. To establish such a relationship, a similarity metric is used to measure how well the images align with each other. Normalized mutual information (NMI) is one of the most commonly used similarity metrics for registering multi-modal images in medical applications [4, 28], therefore we chose this similarity metric. The best match (i.e. between two images) results from reaching the maximum normalized mutual information. To define normalized mutual information, we first need to define entropy of an image. The entropy of image X is

$$ENTROPY(X) = - \sum p_i \log_2 p_i. \quad (1)$$

In this equation p_i is the probability of intensity i occurring in image X. Now we can define the normalized mutual information between two images X and Y:

$$NMI(X, Y) = \frac{ENTROPY(X) + ENTROPY(Y)}{ENTROPY(X, Y)} \quad (2)$$

To calculate $ENTROPY(X, Y)$, the joint entropy of images X and Y, the joint histogram of these two images is needed. For our purposes, X is the 4D Flow MRI dataset and T(Y) is the transformed 3D cine MRI dataset. We would like to find the best rigid transformation T that maximizes $NMI(X, T(Y))$, i.e.

$$\max NMI(X, T(Y)). \quad (3)$$

A solution to this problem can be obtained by iterating over all possible transformations to find the transformation matrix which maximizes the similarity metric between the fixed image and the transformed moving image. Based on the complexity of the datasets and the time needed for iterating over all possible transformations, this problem is a non-linear optimization problem (refer to Equations 1 and 2); therefore, we need to use iterative methods to solve it. Using some kind of optimization method reduces the computation time for solving the registration problem. We chose to use gradient descent to solve the optimization in Equation 3, as it is simple and easy to use [21, 30]. At each iteration, a rigid transformation T is applied to the moving image (3D cine MRI) to map it to the fixed image (4D Flow MRI) and then the similarity measure is calculated between them. The final transformation resulting from the optimization which maximizes NMI can be applied to the 3D cine MRI dataset to align it with the 4D Flow MRI dataset, therefore providing high-resolution anatomical structure data that is properly aligned with the 4D Flow MRI.

4. RESULTS AND EVALUATION

Our method has been applied to 30 pairs of corresponding 3D cine MRI and 4D Flow MRI volumes which represent one cardiac cycle. To match the corresponding time frames between two datasets, an expert clinician picked the volumes that represent late diastole from each dataset. After matching one time frame, correspondence

between the rest of the volumes is simple as the temporal resolution is the same between the two datasets. Since each pair of volumes correspond to the same time frame, the registration is rigid (i.e. composed of rotation and translation).

Fig. 7 shows the result of registering the 3D cine MRI to the 4D Flow MRI after using a three-sketch localization mask (using the left ventricle as the ROI). Qualitatively, it is visible that the corresponding structures match each other well. The short-axis 3D cine MRI has been reoriented based on the registration results to match the 4D Flow MRI which was captured as long-axis images.

Aside from a visual check, a quantitative evaluation of registration has been done using the following metrics: Dice coefficient (DICE), Hausdorff Distance (HD), True Positive Rate (TPR) and True Negative Rate (TNR) [34, 35]. The DICE measures the overlap between two corresponding segmentations S_g and S_t (S_g is the ground truth segmentation of the 4D Flow MRI and S_t is the transferred ground truth segmentation of the 3D cine MRI).

$$DICE = \frac{2 |S_g \cap S_t|}{S_g + S_t} \quad (4)$$

It ranges between 0 and 1: 0 indicates no overlap and 1 indicates complete overlap. The HD measures the maximum distance between the closest points of two segmentations:

$$HD = \max(d(S_g, S_t)) \quad (5)$$

where d indicates the Euclidean distance between the corresponding points of two segmentations. TPR measures the ratio of the overlapped voxels of S_g and S_t to the total voxels of the ground truth segmentation (S_g):

$$TPR = \frac{TP}{TP + FN} \quad (6)$$

where TP is the number of true positive voxels and FN is the number of false negative voxels. TNR measures the ratio of the overlapped voxels in the background of S_g and S_t to the background voxels of the ground truth (S_g):

$$TNR = \frac{TN}{TN + FP} \quad (7)$$

where TN is the number of true negative voxels and FP is the number of the false positive voxels.

To apply the metrics for evaluating registration, manual segmentations (ground truth) have been provided by an expert clinician, for all time frames of the 3D cine MRI and the 4D Flow MRI. The metrics are calculated between S_{gi} and S_{tj} to measure the alignment between each pair of volumes.

Table 1. Evaluation of the registrations using different masks and number of iteration

Mask#iteration	DICE	HD _{mm}	TPR	TNR	Time
manual₂₅₀	0.870	5.353	0.910	0.998	28.8s
three-sketch₂₅₀	0.862	5.498	0.895	0.998	30.6s
single-sketch₅₀₀	0.818	7.277	0.829	0.997	52.4s
box₅₀₀	0.003	36.484	0.006	0.989	55.1s
box₁₀₀₀	0.310	23.156	0.321	0.992	1m40s
box₂₀₀₀	0.775	7.143	0.823	0.996	3m16s

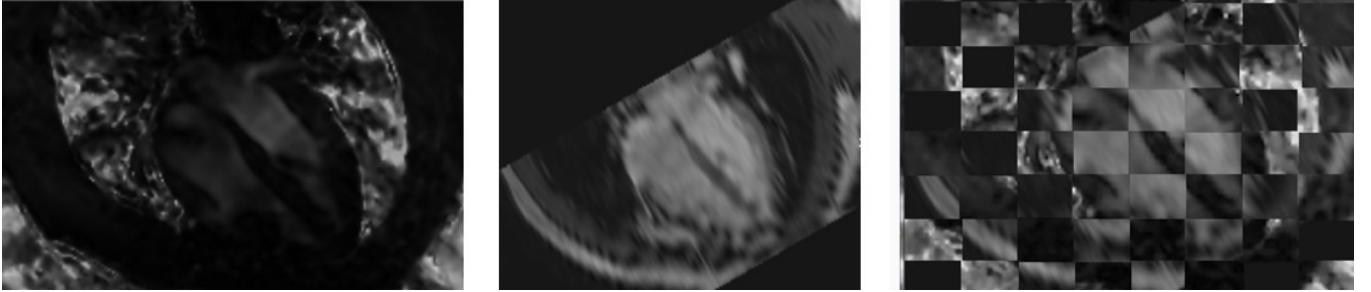


Figure 7. 4D Flow MRI on the left, registered 3D cine MRI to the 4D Flow MRI (middle image), Results of the image registration using the checkerboard visualization for result of the registration of 4D Flow MRI together with the 3D cine MRI.

To evaluate our registration technique we compared the results of registration using four different masks. The masks used for the registrations were (1) the manual segmentation (ground truth) of the left ventricle (S_g), (2) a three-sketch localization around the LV created with our method, (3) a single-sketch mask around the whole heart created with our method, and (4) a bounding box around the heart. Table 1 presents the results of the evaluation, averaged over the 30 pairs of volumes registered.

Based on these results, we note that the quality of the registration using a three-sketch mask is comparable to using the manual segmentation as a mask with the same number of iterations. Increasing the number of iterations does not affect the result of the registration for these two cases. Using a single-sketch mask for registration can result in a good quality registration as well but requires 500 iterations, which is more than both the three-sketch mask and the manual segmentation. Additionally, the registration result is marginally different as noted by the slightly lower DICE and higher HD (Table 1). Finally, using a box as a mask for the registration with 500 iterations results in a poor registration (i.e. a DICE of almost 0). A visual check shows that the right ventricle was incorrectly registered to the left ventricle (Fig. 8). Increasing the number of iterations improves the registration result; experimentally, to obtain a registration of similar quality as using the single-sketch mask, at least 2000 iterations is required (which takes 3m16s on average). Hence, although using a box around the heart as a mask can result in a good quality registration which is visually similar to using the manual segmentation as a mask for registration, it is significantly more time-consuming when compared to the single-sketch, three-sketch or manual segmentation masks. Although the time to register a single time frame does not seem significantly different between using the

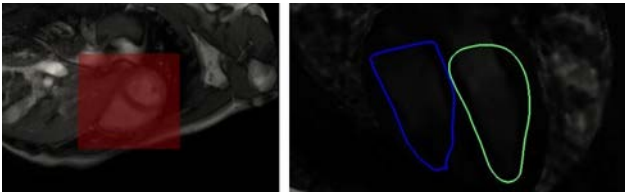


Figure 8. An example of failed registration using a box mask (left) with 500 iteration, blue contour depicts the transferred segmentation compared to the 4D Flow ground truth segmentation shown in green (right).

different localization masks, this increase in time is linear in the number of time frames and the number of datasets to be registered. For example, using a box with 2000 iterations compared to a three-sketch mask with 250 iterations for 30 time frames of data takes at least 1.5 hours and 15 minutes in total, respectively.

In summary, the metrics shown in Table 1 demonstrate that our proposed three-sketch localization technique performs similarly to using a manual segmentation as a localization mask, in terms of both quality and processing time. Moreover, it is faster to draw three rough sketches than to contour over every slice. Using our proposed single-sketch mask can likewise result in a fairly high quality registration, at the cost of slightly more processing time; however, drawing a single rough sketch is arguably even faster than drawing three sketches. Finally, using a box mask for localization leads to significantly higher processing times (more than 3x than using a single-sketch mask), which is undesirable when registering many datasets.

Now that we have registered the 3D cine MRI to the 4D Flow MRI, this data fusion can help in making the anatomical context clearer. Based on the application one can visualize the flow with glyphs or any other common techniques such as streamlines, pathlines, etc [8]. In this paper we used streamlines [26] to visualize the flow inside the left ventricle with either the 4D Flow MRI or the registered 3D cine MRI as the background. As Fig. 9 depicts, the data fusion makes the anatomical context clearer for the corresponding flow.

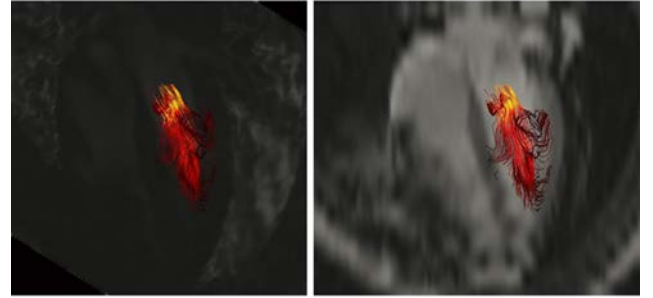


Figure 9. Understanding anatomical context of flow inside the left ventricle (visualized with streamlines) using the magnitude image of the 4D Flow MRI (left) is quite challenging when compared to using the registered 3D cine MRI for context (right).

5. CONCLUSION AND FUTURE WORK

The presented method creates a localization mask for improving registration between 4D Flow MRI and 3D cine MRI for the purpose of aligning the anatomical structure (more clearly detected in 3D cine MRI) to the flow data acquired using 4D Flow MRI. The rough localization mask is constructed by sketch-based user interaction. An intensity-based registration of the 3D cine MRI to the 4D Flow MRI results in a transformation that can be used to transfer the anatomical context to the 4D Flow MRI. As the

localization method is interactive, this method can work with a variety of datasets such as data with noise, low contrast, fuzzy edges, etc.

Based on the results presented in this paper, we attempt to answer the question of “which localization mask is appropriate for registration of cardiac images?” (see Fig. 2). To answer this question, we have shown that if there is a manual segmentation available then it can be used as a localization mask and the quality of results will be good. However, providing a manual segmentation is tedious and time-consuming work. Instead, by just providing three sketches on a single time frame of data, a registration with the same quality can be achieved in the same amount of time. This registration can also be done by simply providing a single rough sketch over the heart; however, slightly more running time is needed for the registration. Therefore, based on the application of how many time frames are going to be registered, one can choose the desired localizing scheme. For example, if only one pair of corresponding volumes are going to be registered then the single-sketch localization mask can be sufficient; otherwise if there are many pairs of time frames to be registered then it is worth creating a three-sketch mask which reduces the overall time compared to the single-sketch mask.

As future work, first, active contours could be used to refine the cross section curve during the curve-constraining step to fit the curve to the data. At this point, we have an appropriate initial state of the curve which helps avoid the problems related to poor initialization of active models (which often end up fitting to the wrong part of the data). This could also be used for segmenting the left ventricle. Second, a non-rigid registration can be considered for providing time-varying segmentation for the 4D Flow MRI.

6. IMPLEMENTATION

The sketch-based interaction and surface construction were implemented by using VTK [31] and C++. The registration was done by using the Elastix [20, 32]. Resulting visualizations were created in ParaView [1].

7. REFERENCES

- [1] James Ahrens, Berk Geveci, Charles Law, C Hansen, and C Johnson. 2005. 36- paraview: An end-user tool for large-data visualization. The visualization hand- book 717 (2005).
- [2] Hung-Li Jason Chen, Faramarz F Samavati, and Mario Costa Sousa. 2008. GPU- based point radiation for interactive volume sculpting and segmentation. The visual computer 24, 7-9 (2008), 689–698.
- [3] Hung-Li Jason Chen, Faramarz F Samavati, Mario Costa Sousa, and Joseph Ross Mitchell. 2006. Sketch-based Volumetric Seeded Region Growing.. In SBM. 123– 129.
- [4] Hua-mei Chen and Pramod K Varshney. 2003. Mutual information-based CT- MR brain image registration using generalized partial volume joint histogram estimation. IEEE Transactions on medical imaging 22, 9 (2003), 1111–1119.
- [5] Joseph Jacob Cherlin, Faramarz Samavati, Mario Costa Sousa, and Joaquim A Jorge. 2005. Sketch-based modeling with few strokes. In Proceedings of the 21st spring conference on Computer graphics. ACM, 137–145.
- [6] André Collignon, Dirk Vandermeulen, Paul Suetens, and Guy Marchal. 1994. Registration of 3D multi-modality medical images using surfaces and point landmarks. Pattern Recognition Letters 15, 5 (1994), 461–467.
- [7] Saul Crandon, Mohammed SM Elbaz, Jos JM Westenberg, Rob J van der Geest, Sven Plein, and Pankaj Garg. 2017. Clinical applications of intra-cardiac four- dimensional flow cardiovascular magnetic resonance: A systematic review. Inter- national journal of cardiology 249 (2017), 486–493.
- [8] Petter Dyverfeldt, Malenka Bissell, Alex J Barker, Ann F Bolger, Carl-Johan Carlhäll, Tino Ebbers, Christopher J Francios, Alex Frydrychowicz, Julia Geiger, Daniel Giese, et al. 2015. 4D flow cardiovascular magnetic resonance consensus statement. Journal of Cardiovascular Magnetic Resonance 17, 1 (2015), 72.
- [9] Mohammed SM Elbaz, Rob J van der Geest, Emmeline E Calkoen, Albert de Roos, Boudewijn PF Lelieveldt, Arno AW Roest, and Jos JM Westenberg. 2017. Assessment of viscous energy loss and the association with three-dimensional vortex ring formation in left ventricular inflow: In vivo evaluation using four- dimensional flow MRI. Magnetic resonance in medicine 77, 2 (2017), 794–805.
- [10] Jonatan Eriksson, Carl Johan Carlhäll, Petter Dyverfeldt, Jan Engvall, Ann F Bol- ger, and Tino Ebbers. 2010. Semi- automatic quantification of 4D left ventricular blood flow. Journal of Cardiovascular Magnetic Resonance 12, 1 (2010), 9.
- [11] Pankaj Garg, Saul Crandon, Peter P Swoboda, Graham J Fent, James RJ Foley, Pei G Chew, Louise AE Brown, Sethumadhavan Vijayan, Mariëlla ECJ Hassell, Robin Nijveldt, et al. 2018. Left ventricular blood flow kinetic energy after myocardial infarction-insights from 4D flow cardiovascular magnetic resonance. Journal of Cardiovascular Magnetic Resonance 20, 1 (2018), 61.
- [12] Pankaj Garg, Rob J van der Geest, Peter P Swoboda, Saul Crandon, Graham J Fent, James RJ Foley, Laura E Dobson, Tarique Al Musa, Sebastian Onciu, Sethumad- havan Vijayan, et al. 2018. Left ventricular thrombus formation in myocardial infarction is associated with altered left ventricular blood flow energetics. Euro- pean Heart Journal- Cardiovascular Imaging (2018).
- [13] Pascale Gerlot-Chiron and Yves Bizais. 1992. Registration of multimodality medical images using a region overlap criterion. CVGIP: graphical models and image processing 54, 5 (1992), 396–406.
- [14] Damien Grosgeorge, Caroline Petitjean, Jérôme Caudron, Jeannette Fares, and Jean-Nicolas Dacher. 2011. Automatic cardiac ventricle segmentation in MR images: a validation study. International journal of computer assisted radiology and surgery 6, 5 (2011), 573–581.
- [15] Vikas Gupta, Mariana Bustamante, Alexandru Fredriksson, Carl-johan Carl- häll, and Tino Ebbers. 2018. Improving left ventricular segmentation in four- dimensional flow Mri using intramodality image registration for cardiac blood flow analysis. Magnetic resonance in medicine 79, 1 (2018), 554–560.
- [16] Joseph V Hajnal and Derek LG Hill. 2001. Medical image registration. CRC press.
- [17] Victoria Härd. 2016. Automatic alignment of 2D cine morphological images using 4D Flow MRI data.
- [18] Vivian P Kamphuis, Mohammed SM Elbaz, Pieter J van den Boogaard, Lucia JM Kroft, Rob J van der Geest, Albert de Roos, Willem A Helbing, Nico A Blom, Jos JM Westenberg, and Arno AW Roest. 2018. Disproportionate intraventricular

- viscous energy loss in Fontan patients: analysis by 4D flow MRI. *European Heart Journal-Cardiovascular Imaging* (2018).
- [19] Vivian P Kamphuis, Jos JM Westenberg, Roel LF van der Palen, Pieter J van den Boogaard, Rob J van der Geest, Albert de Roos, Nico A Blom, Arno AW Roest, and Mohammed SM Elbaz. 2018. Scan–rescan reproducibility of diastolic left ventricular kinetic energy, viscous energy loss and vorticity assessment using 4D flow MRI: analysis in healthy subjects. *The International Journal of Cardiovascular Imaging* (2018), 1–16.
- [20] Stefan Klein, Marius Staring, Keelin Murphy, Max A Viergever, and Josien PW Pluim. 2010. Elastix: a toolbox for intensity-based medical image registration. *IEEE transactions on medical imaging* 29, 1 (2010), 196–205.
- [21] Lok Wan Lorraine Ma. 2016. Mathematical methods for 2D-3D cardiac image registration. Ph.D. Dissertation.
- [22] Frederik Maes, Andre Collignon, Dirk Vandermeulen, Guy Marchal, and Paul Suetens. 1997. Multimodality image registration by maximization of mutual information. *IEEE transactions on Medical Imaging* 16, 2 (1997), 187–198.
- [23] Filip Malmberg, Richard Nordenskjöld, Robin Strand, and Joel Kullberg. 2017. SmartPaint: a tool for interactive segmentation of medical volume images. *Computer Methods in Biomechanics and Biomedical Engineering: Imaging & Visualization* 5, 1 (2017), 36–44.
- [24] Michael Markl, Alex Frydrychowicz, Sebastian Kozerke, Mike Hope, and Oliver Wieben. 2012. 4D flow MRI. *Journal of Magnetic Resonance Imaging* 36, 5 (2012), 1015–1036.
- [25] Hiba A Mohammed. 2016. The Image Registration Techniques for Medical Imaging (MRI-CT). *American Journal of Biomedical Engineering* 6, 2 (2016), 53–58.
- [26] Sandy Napel, Donald H Lee, Richard Frayne, and Brian K Rutt. 1992. Visualizing three-dimensional flow with simulated streamlines and three-dimensional phase-contrast MR imaging. *Journal of magnetic resonance imaging* 2, 2 (1992), 143–153.
- [27] Shigeru Owada, Frank Nielsen, Takeo Igarashi, Ryo Haraguchi, and Kazuo Nakazawa. 2008. Projection plane processing for sketch-based volume segmentation. In *2008 5th IEEE International Symposium on Biomedical Imaging: From Nano to Macro*. IEEE, 117–120.
- [28] Josien PW Pluim, JB Antoine Maintz, and Max A Viergever. 2003. Mutual-information-based registration of medical images: a survey. *IEEE transactions on medical imaging* 22, 8 (2003), 986–1004.
- [29] Karl Rohr. 2000. Elastic registration of multimodal medical images: A survey. *KI14*, 3 (2000), 11–17.
- [30] Sebastian Ruder. 2016. An overview of gradient descent optimization algorithms. *arXiv preprint arXiv:1609.04747* (2016).
- [31] Will J Schroeder, Bill Lorensen, and Ken Martin. 2004. The visualization toolkit: an object-oriented approach to 3D graphics. Kitware.
- [32] Denis P Shamonin, Esther E Bron, Boudewijn PF Lelieveldt, Marion Smits, Stefan Klein, and Marius Staring. 2014. Fast parallel image registration on CPU and GPU for diagnostic classification of Alzheimer’s disease. *Frontiers in neuroinformatics* 7 (2014), 50.
- [33] Miguel Souto, Lambert Raul Masip, Miguel Couto, Jorge Juan Suárez-Cuenca, Amparo Martínez, Pablo G Tahoces, Jose Martin Carreira, and Pierre Croisille. 2013. Quantification of right and left ventricular function in cardiac MR imaging: comparison of semiautomatic and manual segmentation algorithms. *Diagnostics* 3, 2 (2013), 271–282.
- [34] Abdel Aziz Taha and Allan Hanbury. 2015. Metrics for evaluating 3D medical image segmentation: analysis, selection, and tool. *BMC medical imaging* 15, 1 (2015), 29.
- [35] Abdel Aziz Taha and Allan Hanbury. 2017. Evaluation Metrics for Medical Organ Segmentation and Lesion Detection. In *Cloud-Based Benchmarking of Medical Image Analysis*. Springer, 87–105.
- [36] Holger Thiele, Eike Nagel, Ingo Paetsch, Bernhard Schnackenburg, Axel Bornstedt, Marc Kouwenhoven, Andreas Wahl, Gerhard Schuler, and Eckart Fleck. 2001. Functional cardiac MR imaging with steady-state free precession (SSFP) significantly improves endocardial border delineation without contrast agents. *Journal of Magnetic Resonance Imaging: An Official Journal of the International Society for Magnetic Resonance in Medicine* 14, 4 (2001), 362–367.
- [37] Rob J van der Geest and Pankaj Garg. 2016. Advanced analysis techniques for intra-cardiac flow evaluation from 4D flow MRI. *Current radiology reports* 4, 7 (2016), 38.
- [38] William M Wells, Paul Viola, Hideki Atsumi, Shin Nakajima, and Ron Kikinis. 1996. Multi-modal volume registration by maximization of mutual information. *Medical image analysis* 1, 1 (1996), 35–51.
- [39] Wu Zhou and Yaoqin Xie. 2013. Interactive medical image segmentation using snake and multiscale curve editing. *Computational and mathematical methods in medicine* 2013 (2013).